*International Journal of Steel Structures* 17(4): 1515-1528 (2017)
DOI 10.1007/s13296-017-1219-4
ISSN 1598-2351 (Print)
ISSN 2093-6311 (Online)

International Journal of
STEEL
STRUCTURES
www.springer.com/journal/13296

# Numerical Analysis on Structural Behaviors of Concrete Filled Steel Tube Reinforced Concrete (CFSTRC) Columns Subjected To 3-side Fire

**Lei Xu[1,2,*], Ming-Tao Wang[2], Yan-Hong Bao[2], and Wen-Da Wang[2]**

[1]*School of Civil Engineering; Dalian Nationalities University, Dalian 116600, China*
[2]*Key Laboratory of Disaster Prevention and Mitigation in Civil Engineering of Gansu Province, Lanzhou University of Technology, Lanzhou 730050, China*

**Abstract**

The structural behaviors of concrete filled steel tube reinforced concrete (CFSTRC) columns, which were exposed to a 3-side fire were discussed by using the non-linear finite element analysis (FEA) software ABAQUS. Details of the temperature distribution, fire resistance, failure modes, redistribution of internal force, contact stress between the steel tube and the concrete (both inside and outside of the steel tube), and the development of stress and strain within the CFSTRC columns subjected to a 3-side fire were revealed. The factors that may have affected the fire resistance of the CFSTRC columns exposed to three-side fire were analyzed. Based on the above research, the present study observed uniaxial symmetry on the cross-sectional thermal distribution of the CFSTRC, wherein a significantly lower temperature on the unexposed side was observed as compared to the exposed side. The two side verges of the surface, which were not exposed to fire, exhibited the lowest temperature. Following the end of the heating, the maximum temperature difference reached about 1065°C. The large temperature difference would bring non-uniform thermal stress and strain, and accidental eccentricity. In addition, the existence of concrete inside and outside of the steel tube prevented the steel tube from occurring local buckling, and the failure modes of CFSTRC columns acted as overall bucking. Parameters such as the fire load ratio, sectional dimension, slenderness ratio, sectional core area ratio, and external concrete compression strength significantly influenced the fire resistance of the CFSTRC columns. Finally, a simplified calculating formula was proposed to calculate the fire resistance influence factors of the CFSTRC columns subjected to three-sid fire. The formula-calculated results were well in agreement with the finite element analysis results, thereby providing a simple and feasible method for evaluating the fire-resistance design of these types of components in practical engineering.

**Keywords:** concrete filled steel tube reinforced concrete (CFSTRC), columns, three-side fire, mechanical behavior, fire resistance, simplified calculation

## 1. Introduction

Concrete filled steel tube reinforced concrete (CFSTRC) consists of inner concrete filled steel tube (CFST) and outer reinforced concrete (RC), as shown in Fig. 1. This kind of structure combines all the advantages of CFST and RC perfectly, so it has a high load bearing capacity, good anti-seismic performance, excellent fireproof property and convenient workability. As a result, CFSTRC columns have been widely applied to high-rise and super high-rise buildings (Hong and Tao, 2005). Along with its extensive application, the fire resistance capacity of CFSTRC columns are drawing attentions from an increasing number of researchers.

For the column in the building structure, the columns are usually in non-uniform fire due to the heat absorption of the wall and the surrounding structure, such as the single side, adjacent sides, opposite sides, and the three surfaces. The reduction in the surface of the fire affected the overall temperature of the column section and the degree of damage of the material to some extent, which is beneficial to the improvement of the fire resistance of the structure. On the other hand, under the condition of single axial symmetry, which is subjected to single-sided fire and three-sided fire, the structure produces asymmetric temperature deformation and additional eccentricity, which may reduce the fire resistance of the structure.

Received November 12, 2016; accepted May 23, 2017;
published online December 31, 2017


*Corresponding author
Tel: +86-11-87557303, Fax: +86-11-87557303
E-mail: xulei@dlnu.edu.cn, xulgb@163.com

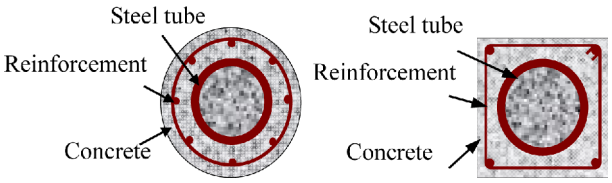


**Figure 1.** Typical cross-sections of CFSTRC columns.

Thus, the mechanism and fire resistance of the columns exposed to non-uniform fire differ from columns under uniform fire, thereby necessitating the understanding of fire resistance for columns under non-uniform fire to generate the corresponding fire resistance design method for the columns. A lot of research has been performed on the fire resistance of columns under non-uniform fire (Guo and Shi, 2003; Wu *et al*., 2007; Li, 2003; Lv *et al*.; 2012; Lv *et al*., 2013; Yang *et al*., 2010). Xu and Liu (2013) and Feng *et al*. (2008) conducted experimental investigations on CFSTRC columns subjected to four-side uniform fire. However, little research has been executed on the fire behavior of CFSTRC columns exposed to non-uniform fire. The present study depicts the typical three-sided fire as the foundation for determining the working mechanism of CFSTRC columns when was subjected to a non-uniform fire.

## 2. Temperature Field of CFSTRC Columns Exposed to Three-side Fire

Thermal distribution is the foundation of researching the mechanical behavior during or after exposure to ISO-834 standard fire, which also, occupies a crucial status in the process of studying the high-temperature mechanical behavior of CFSTRC columns. In this paper, in view of the costly test fees, the non-linear finite element analysis (FEA) software ABAQUS was used to establish the thermal analysis model of CFSTRC columns. By using it, the characteristics of temperature distribution and the tendency of temperature variation in a three-surface fire are discussed.

### 2.1. Thermal properties of steel and concrete

The determination of the thermal properties of steel and concrete is the precondition for determining the temperature field of a CFSTRC column, which include the thermal expansion coefficient, thermal conductivity, and specific heat, all of which are functions of the temperature. In this paper, the expressions proposed by Canadian scholar Lie (1994) were selected. When calculating the specific heat capacity of concrete, the influence of water vapor is considered, which possess preferable calculation accuracy.

### 2.2. Temperature field finite element analysis model and verification

When creating the thermal analysis model, 8-node linear heat transfer brick (DC3D8) is adopted to simulate concrete and steel tube, 2-node heat transfer link (DC1D2) is used for steel bars. The influence of convection and radiation must be reckoned in, and the heat convective coefficient of the fire side is taken as 25 W/(m$^2$·ºC), the adiabatic surface taken as 9 W/(m$^2$·ºC); the surface radiation emissivity is selected as 0.5 (ECCS 1998); the contact between the tube and concrete is 'Tie' constraint provided by ABAQUS analysis platform; the 'Tie' constraint is also used for simulating the contact between reinforcing cage and exterior concrete. The initial temperature and the absolute zero temperature were defined as 20 and –273ºC respectively, and Stefan-Boltzmann constant were set to be 5.67e-8 W/(m$^2$·K$^4$). The CFSTRC column is heated according to ISO-834 standard fire curve.

In order to verify above thermal analysis model, experimental data from Lie *et al.* (1984) and Lie and Chabot (1992) are extracted to compare with the calculation results, which shown in Fig. 2. In Fig. 2, symbol *d* denotes the distance from the kernel of section to the peripheral concrete surface. It can be seen from the Fig. 2 that the predicted temperatures have a fairly good agreement with those of measured.

### 2.3. Temperature distribution of CFSTRC columns subjected to three-side fire

At present, there's little experimental investigation on

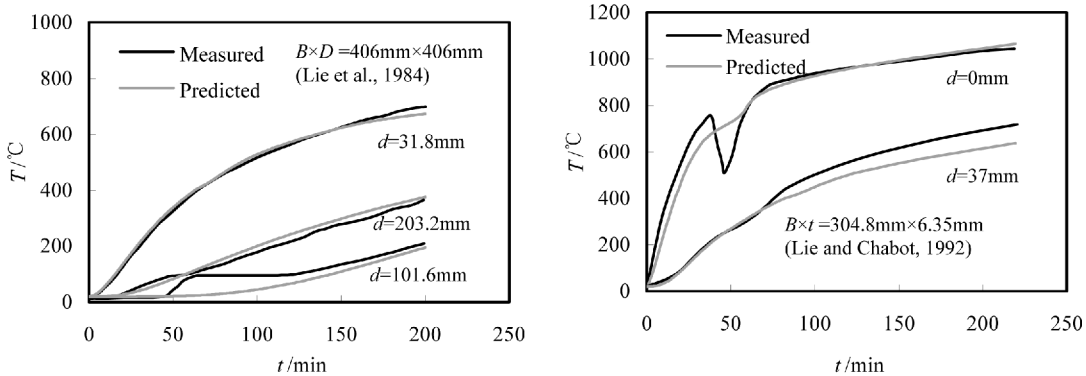


(a) Reinforced concrete columns (b) Concrete filled steel tube columns

**Figure 2.** Comparison of *T-t* curves between predicted and measured results for RC and CFST column.

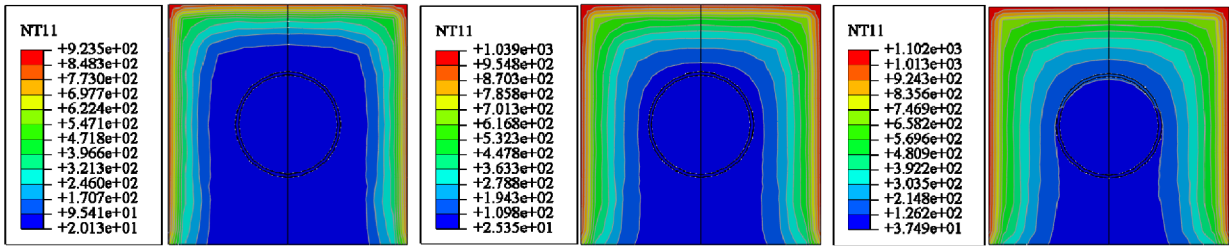


(a) t=60 min (b) t=120 min (c) t=180 min

**Figure 3.** Temperature distribution of CFSTRC column at different moments subjected to 3-side fire.

the fire performance of CFSTRC column under non-uniform fire conditions. In order to know the temperature distribution of CFSTRC column subjected to three-side fire extensively, a typical CFSTRC member was established with the aid of ABAQUS software. The detailed parameters as follows: the column have dimensions of $B \times D \times t \times L$ = 500×220×6×5800 (mm), where $B$ is the width of cross-section, $D$ and $t$ are the diameter and thickness of steel tube, $L$ is the length of column; concrete strength both inside and outside the tube are C60 ($f_{cu}$=60 MPa); the steel tube adopts Q345 ($f_y$=345 MPa); the layout of longitude bar is 16Φ20 ($f_y$=400 MP), and for stirrup is $\varphi$8@100 ($f_y$=300 MP). Figure 3 shows the temperature distribution of the CFSTRC column sections at different three-surface fire heating times, where, NT11 represents the node temperature, and the fire exposing time is 180 minutes.

As can be seen from the above diagram that the thermal distribution appears to be mono-symmetrical and the lowest temperature was observed in the nearby region of the unexposed surface. The temperature of the unexposed surface was significantly lower than those of the other three surfaces. At the end of the heating,a maximum temperature difference of about 1065ºC was observed. The large temperature difference can induce non-uniform thermal stress and strain in the cross section, thereby generating an eccentric rotation of intensity center of the cross section (Lv, 2010), which is adverse to the fire performance of CFSTRC column. For those CFSTRC columns subjected to 3-side fire, temperature varies drastically at the corner of the outside concrete than other zones.

## 3. Mechanical Behavior of CFSTRC Columns Subjected to Three-side Fire

On the foundation of above thermal analysis, the method of "successive thermal-stress coupling analysis" was adopted to analyze the structural behaviors of the CFSTRC column under 3-side fire (as shown in Fig. 4). Firstly, the load was gradually applied to the design value at the ambient temperature, after which the temperature field results calculated above were imported, during heating, keeping the load unchanged until the failure of columns occurred.

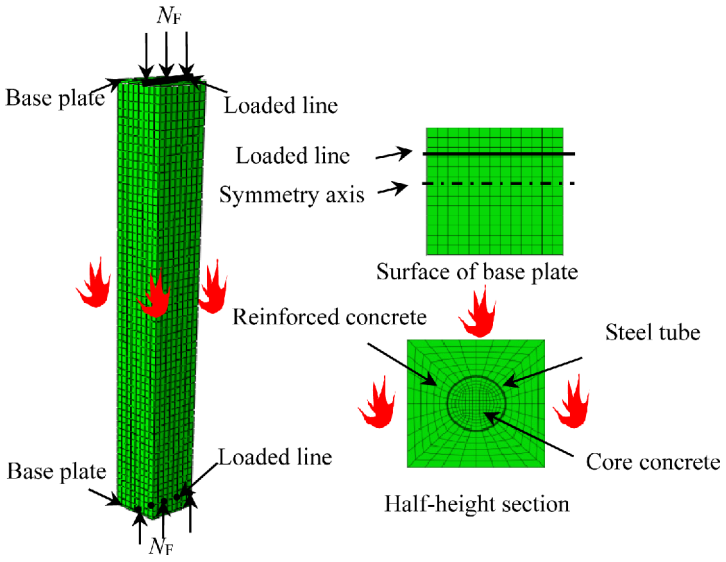


**Figure 4.** Finite element analysis model of CFSTRC column subjected to 3-side fire.

### 3.1. Thermodynamic constitutive model of CFSTRC columns at high temperature

To analyze the fire behavior of CFSTRC columns exposed to high temperature, reasonable stress-strain relation of concrete and steel should be selected. For steel, we adopted the formula put forward by Lie (1994), which has been adopted by many scholars. Specific expressions are presented in Formula 1. Figure 5 presents the stress-strain relation of steel (Q345) calculated by this fomula at different temperatures.

$$\sigma_s=\begin{cases}\dfrac{f(T,0.001)}{0.001}\varepsilon_s & \varepsilon_s\le\varepsilon_p\\ \dfrac{f(T,0.001)}{0.001}\varepsilon_p+f\left[\left(T,(\varepsilon_s-\varepsilon_p+0.001)\right]\right]-f(T,0.001) & \varepsilon_s>\varepsilon_p\end{cases} \tag{1}$$

where $T$ is the current temperature in°C;

$\varepsilon_p=4\times10^{-6}f_y$; $f(T,0.001)=(345-0.276T)\times\left\{1-e^{[(-30+0.03T)]\sqrt{0.001}}\right\}$;

$f\left[T,(\varepsilon_s-\varepsilon_p+0.001)\right]=\left\{1-e^{[(-30+0.03T)\sqrt{\varepsilon_s-\varepsilon_p+0.001}]}\right\}\times(345-0.276T)$.

On account of confination between steel tube and infilling concrete, the peak stress and strain of inner core concrete increase in certain degree, therefore, we used the expression proposed by Professor Han (2007), the specific expressions of which are presented in Formula 2. Figure 6 shows the stress-strain relation of inner concrete (C60) calculated by Han's model. Given that peripheral concrete is unrestricted concrete, the present study choose the formula proposed by Lie and Denham (1993), the specific expressions of which are presented in Formula 3. Figure 7 shows the stress-strain relation of the outer concrete (C60) calculated by Lie's formula.

$$y=\begin{cases}2x-x^2 & x\le1\\ \dfrac{x}{\beta(x-1)^2+x} & x>1\end{cases};\ x=\frac{\varepsilon}{\varepsilon_0^{\ T}};\ y=\frac{\sigma}{\sigma_0^{\ T}};$$
$$\sigma_0^{\ T}=f_c'\Big/\left[1+a\left(\frac{T-20}{1000}\right)^b\right];a=0.017f_c'+7.83;b=-0.016f_c'+3.77; \tag{2}$$

$$\varepsilon_0^{\ T}=\varepsilon_c(T)+800\cdot\xi^{0.2}\cdot10^{-6}\cdot\left[1+0.18\times\left(\frac{T-20}{100}\right)^{2.2}\right]$$
$$\varepsilon_c(T)=(1300+12.5f_c')\cdot10^{-6}\cdot\left[1+0.18\times\left(\frac{T-20}{100}\right)^{2.2}\right]$$
$$\beta=\left(2.36\times10^{-5}\right)^{\left[0.25+(\xi-0.5)^2\right]}\times(f_c')^{0.5}\times0.5;$$
$$\xi=A_sf_y(T)/A_cf_{ck}$$

where $T$ is the temperature in °C; $f_c'$ is the compressive strength of the concrete cylinder in MPa; $A_s$ and $A_c$ are the cross-sectional areas of steel and concrete, respectively; $f_y(T)$ is the yield strength of steel under temperature $T$, and $f_{ck}$ is the standard value of the axial compressive strength of concrete.

$$\sigma_c=\begin{cases}f_c'(T)[1-(\dfrac{\varepsilon_{oh}-\varepsilon_c}{\varepsilon_{oh}})^2] & \varepsilon_c\le\varepsilon_{oh}\\ f_c'(T)[1-(\dfrac{\varepsilon_c-\varepsilon_{oh}}{\varepsilon_{oh}})^2] & \varepsilon_c>\varepsilon_{oh}\end{cases} \tag{3}$$

where $\varepsilon_{oh}=0.0025+(6T+0.04T^2)\times10^{-6}$;

$$f_c'(T)=\begin{cases}f_c' & 0℃<T\le450℃\\ f_c'[2.011-2.353(\dfrac{T-20}{1000})] & 450℃\le T\le874℃\\ 0 & T>874℃\end{cases}$$

where, $\sigma_c$ and $\varepsilon_c$ are the stress and strain of the concrete, respectively; $\varepsilon_{oh}$ is the peak strain of the concrete, and $f_c'(T)$ is the compressive strength of the concrete cylinder at temperature $T$.

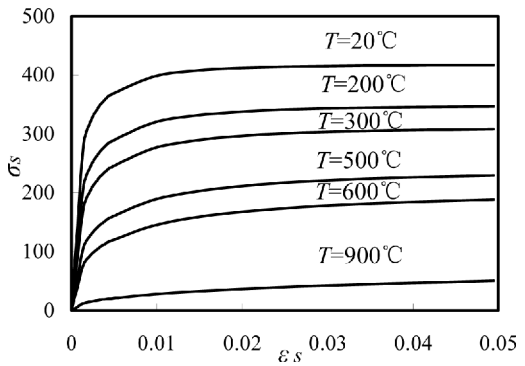


**Figure 5.** Stress-strain relation of steel at different temperatures.

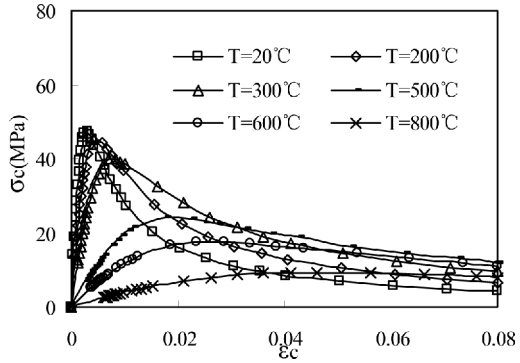


**Figure 6.** Stress-strain relation of infilling concrete at different temperatures.

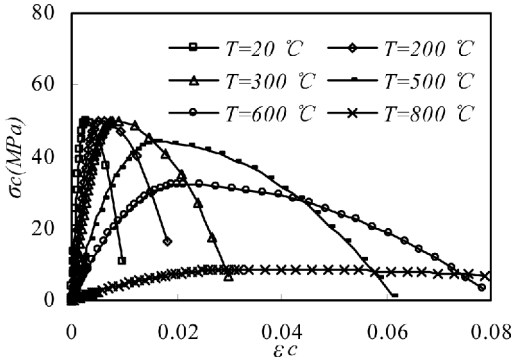


**Figure 7.** Stress-strain relation of peripheral concrete at different temperatures.

### 3.2. Establishment and verification of mechanical analysis model

When set up the mechanic analysis model under ISO-834 standard fire, the concrete and steel tube employed an 8-node linear heat transfer brick (DC3D8), and the steel bars adopts 2-node heat transfer link (DC1D2) elements. In addition, the two sub-plates at the ends of column with high stiffness (set the element type as DC3D8) were employed to simulate the loading plates of the CFSTRC column. In the process of calculation by using the mechanical analysis model at high temperature, the serial number of each node in elements and mesh size must be consistent with the thermal analysis model in order to ensure each node's temperature can be read correctly.

Contact problem is crucial in the finite element analysis, as this directly influences the precision and convergence property of calculation results. In the model, the contact between steel tube and concrete , specifically both inside and outside of the tube adopted "Hard Contact" in the normal direction, given that the interface is able to transfer compressive stress completely and incapable of transferring the tensile stress. In the tangent direction, the Coulomb friction model was used to simulate the transmission of tangential force (Hibbitt *et al.*, 2007), setting the friction coefficient as 0.6 (Han, 2007). Supposed that the steel bars and peripheral concrete fully bonded and have the equal temperature in the same geometry coordinate point, so "Tie" constraint is adopted. Wherein the bottom of the CFSTRC column, exhibits restraint in the displacement of x, y, z three directions, that is, U1=U2=U3=0; and the top of the column, exhibits restraint in the displacement of x, y direction, releasing the displacement of z direction.

Experimental data of CFST and SRC columns subjected to 3-side fire are collected from Lv (2010), Liu (2010) and Li (2011) respectively to verify the availability of the high-temperature mechanical performance analysis model at high temperature established above, the calculated results are compared with those of measured, which shown in Figure 8. It can be seen from the Figure 8 that the results of simulation are good agree with those of experiments.

### 3.3. mechanical behaviour of CFSTRC columns subjected to three-side fire

To understand the internal mechanism of the destruction and mechanical essence of CFSTRC columns at high temperature clearly, the typical CFSTRC column created in section 2.3 and the mechanical analysis model established in section 3.2 are adopted to analyze the failure modes, fire endurance, redistribution of internal force, the development of stress and strain and the contact stress between steel tube and concrete of CFSTRC columns subjected to 3-side fire.

A square cross-sectional CFSTRC column was adopted as the sample column for the analysis. It exhibited a cross-sectional height ($B$) of 500 mm, an outer steel tube diameter ($D$) of 220 mm, a steel tube thickness ($t$) of 6 mm, and a component height ($H$) of 5800 mm, of which the whole height was fired. The cube compression strength of the concrete ($f_{cu}$) both inside and outside of the steel tube was measured at 60 MPa, the yield strength of steel was 345 MPa, and the sectional core area ratio ($a_{sc}$) was 0.15, wherein $a_{sc}$ is defined as $A_{sc}/A_0$, where $A_{sc}$ is the cross-sectional area of the core CFST and $A_0$ is the cross-sectional area of total cross section. In addition, 16Φ20 steel bars were used as the longitudinal bars, which had a yield strength ($f_{yb}$) of 400 MPa and a reinforcement ratio ($\rho_b$) of 1.78%. $\varphi$10 steel bars were used as the stirrups in the columns, which exhibited a yield strength ($f_{yb}$) of 300 MPa. The stirrup spacing was set at 100 mm and the slenderness ratio ($\lambda$) was set at 40, which was calculated by $\lambda = 2\sqrt{3}L/B = 12$. The eccentricity was 125 mm; the eccentricity ratio $e/r_0$ was 0.5, including $r_0 = B/2$; and the column load ratio ($n$) was 0.6, wherein $n$ is defined as $N_F/N_u$ such that $N_F$ is the load on the column in fire and $N_u$ is the axial compressive capacity of column at ambient temperature. The present study had a $N_u$ value of 3852 kN.

The present study adopted the failure criteria specified in ISO-834 (1999) for the columns. The column was axially contracted by $0.01H$ mm and at a rate of contraction that reached $0.003H$ mm/min, where $H$ is the calculating length of the column in mm.

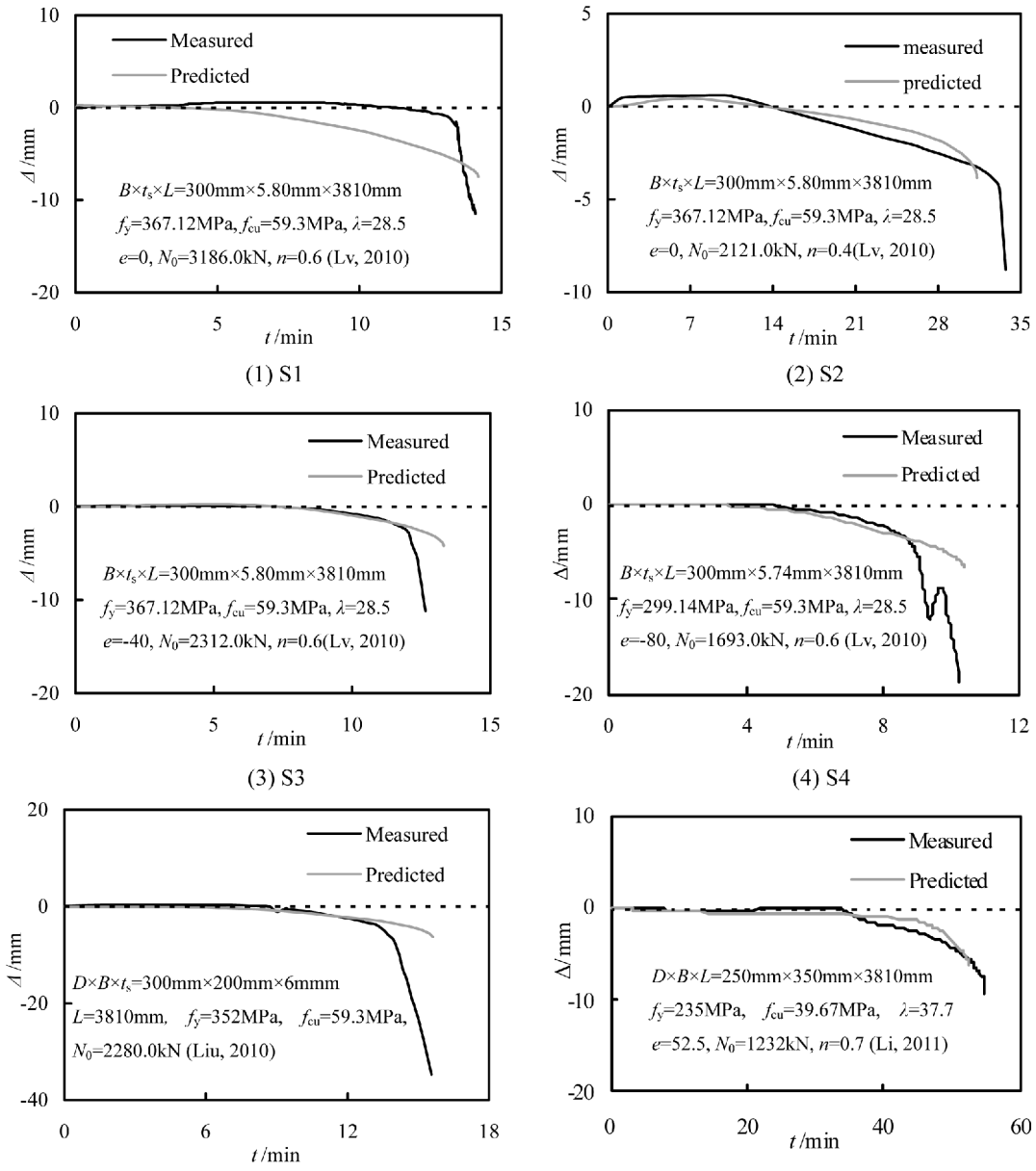


(a) Concrete filled steel tube columns (b) Steel reinforced concrete

**Figure 8.** Comparison of axial deformation of CFST and SRC columns subjected to 3-side fire.

(a) Failure modes of the CFSTRC column

Figure 9 shows the failure mode of the CFSTRC column subjected to 3-side fire, in order to show clearly, we magnify the deformation by 3 times. As can be seen from Fig. 9 that the failure mode of the CFSTRC column exhibits overall bucking, and the existence of concrete inside and outside the steel tube prevented the steel tube from happening local buckling effectively.

(b) Axial and lateral deformation of the CFSTRC column

The axial and lateral deformation versus time curves of typical CFSTRC columns subjected to 3-side fire are given in Fig. 10, where, abscissa axis is fire exposing time, vertical axis are axial displacement and half-height deflection respectively.

It can be seen from Fig. 10(a) that the axial deformation-time curve of CFSTRC columns subjected to 3-side fire can be divided into three parts: (I) expansion phase, (II) gradually decline phase, and (III) sudden drop phase. In the first phase, which exhibits a short heating time of about 2 minutes, the heat absorption of the column increases and the degradation of the material is slight, thereby expanding the axial deformation. With the increase of the fire time, the axial deformation with the fire time curves go into the second phase, wherein the heat absorbed by

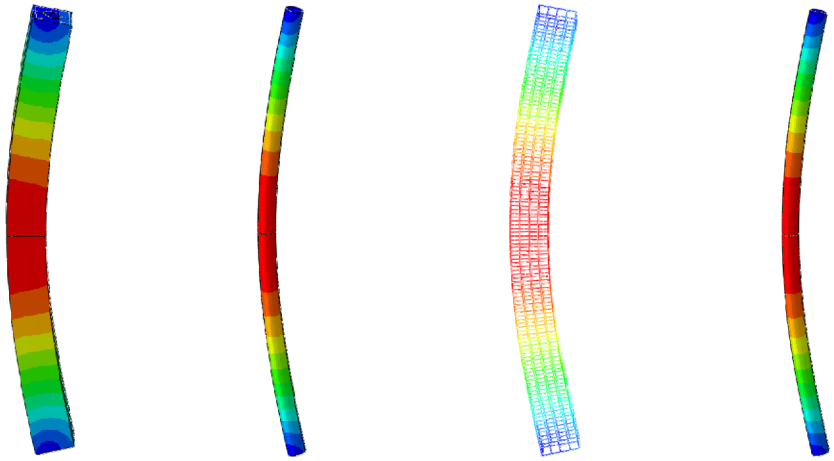

(a) Outside concrete (b) Steel tube (c) reinforcement cage (d) inner concrete

**Figure 9.** Failure modes of each component subjected to 3-side fire.

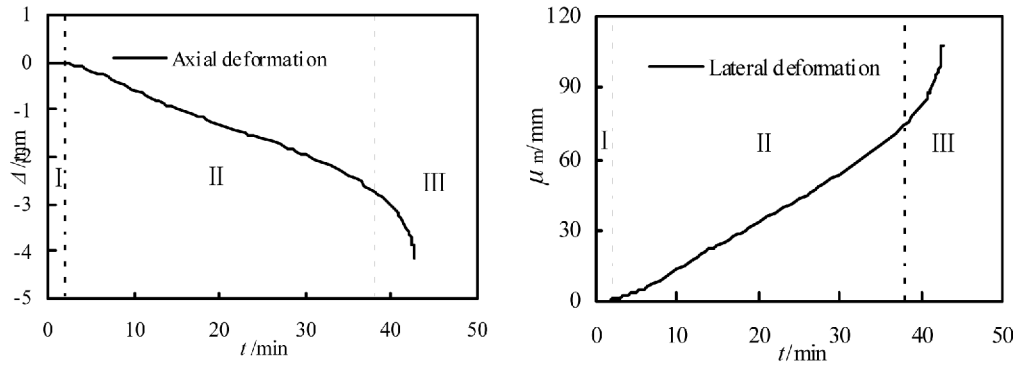


(a) Axial deformation (b) Half-height deflection

**Figure 10.** The deformation-time curves of CFSTRC columns subjected to 3-side fire.

the component increases and the temperature of the column increases, thereby deteriorating the mechanical properties of the material. Under the combined action of the load, the column exhibited a greater axial deformation rate greater than that of the first stage and remained almost constant. The axial deformation of the column increased with the increase of the fire time. When the axial deformation of the column increased sharply, the axial deformation of the column entered the failure stage due to the deterioration of the material in most areas of the column section. Under the joint action of the two order effects, the column eventually lost its bearing capacity and failed.

The lateral deformation-time curve of the CFSTRC column subjected to 3-side fire is presented in Fig. 10(b). As with the axial deformation, the lateral deformation curves were also divided to three stages. In the first phase, due to the limited heat absorption, the column still has the very good integrity, the deflection of mid-height remains unchanged basically. As it moved into the second stage, the property of each component becomes retrogressive, coupled with the "second order moment effect" caused by eccentric loading, the mid-span deflection increased unremittingly; In the last phase, the column failed due to lose its stability. From the Figure 10(b), As the column was ultimately destroyed, as presented in Figure 10(b), the half-height deflection of the columns significantly increased, which conforms with the appearance of overall buckling failure.

(c) The redistribution of axial forces

The CFSTRC column generated an inconsonant temperature stress and thermal expansion deformation in the presence of non-uniform fire condition due to the differences in the specific heat capacity, density, thermal expansion coefficient, and thermal conductivity of each component. At the same time, the degradation degree of the material performance at high temperatures was not consistent and generated internal force redistribution.

Figure 11 presents axial force changes over time. Extensions to the heating time resulted in constant axial force adjustments for each group in the CFSTRC column constantly. During the initial fire period, the temperature of the outer reinforced concrete was much higher than other components, thereby producing greater thermal expansion deformation and acquiring more axial force.

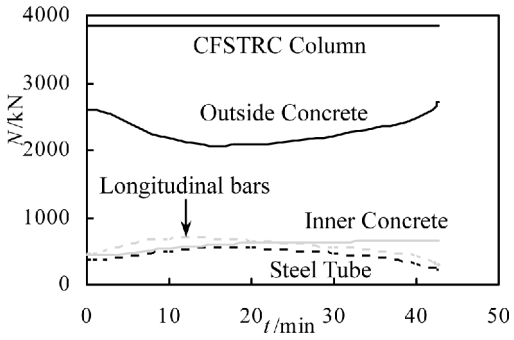


**Figure 11.** The redistribution of axial force subjected to three-faces fire.

Similarly, the internal force accepted by the other components decreased in the presence of invariable external loads. About 1 min after, the strength and rigidity of the outer concrete weakened, thereby gradually transferring the generated load inward to the longitudinal bars such that the load on the external concrete began to fall and the load on the longitudinal reinforcement increased. Following an increase in the fire time, the heat was gradually transferred from the outside to the inside, and approximately 12 min later, the longitudinal reinforcement also deteriorated, which in turn transferred the load of the steel bar to the internal section of the outer concrete and the concrete filled steel tube. The load of the external concrete and interior concrete filled steel tube began to increase due to the increase in the half-height deflection. Given that most of the steel tube is in the tensile zone, the external load of the steel tube was then reduced.

(d) The change and development of strain

Figure 12 presents the distribution of the longitudinal strain on the half-height section of the CFSTRC columns at different heating times, wherein the longitudinal strain (LE33) of both the compressive and tensile zones increased following an extension of the fire exposing time. In addition, the growth velocity on the tensile side more rapidly increased than on the pressure side. Meanwhile, the neutral axis constantly moved towards the pressure side and the area of compressive zone gradually decreased. On the contrary, the increasing area observed in the tensile region. As the column reached its fire endurance maximum, the area of tensile zone exhibited 45% that of the total cross-sectional area.

At the same time, the half-height section exhibited homogeneous zonal longitudinal strain distribution along the height of the section before heating. As the time went on, the distribution of the longitudinal strain in the compressive zone became uneven. As the column was close to reaching its fire endurance, the distribution of the longitudinal strain on both the compressive zone and the tensile region became cratered and shapeless.

(e) The change and development of stress

Figure 13 shows the development and change of stress on the mid-height section of the CFSTRC columns subjected to 3-side fire, wherein $f_c'$ is the compressive strength of concrete at normal temperature.

Based on Fig. 13, under an eccentric load, the longitudinal stress (S33) presented homogeneous zonal distribution along the height of the section before heating, with one

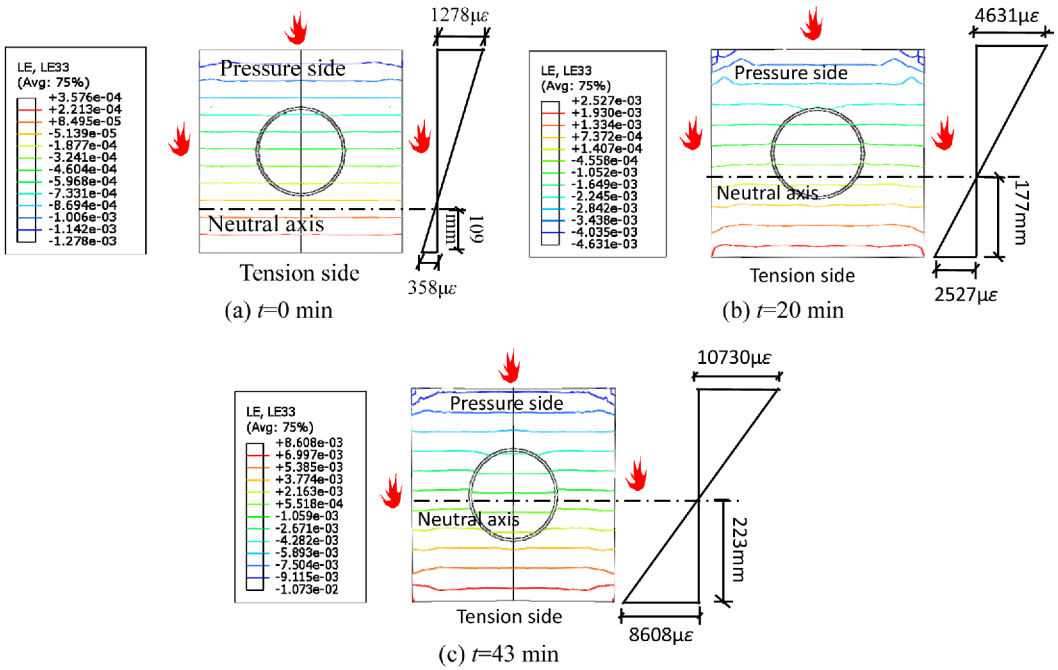


**Figure 12.** Development and change of longitudinal strain (LE33) on mid-span section at different moments

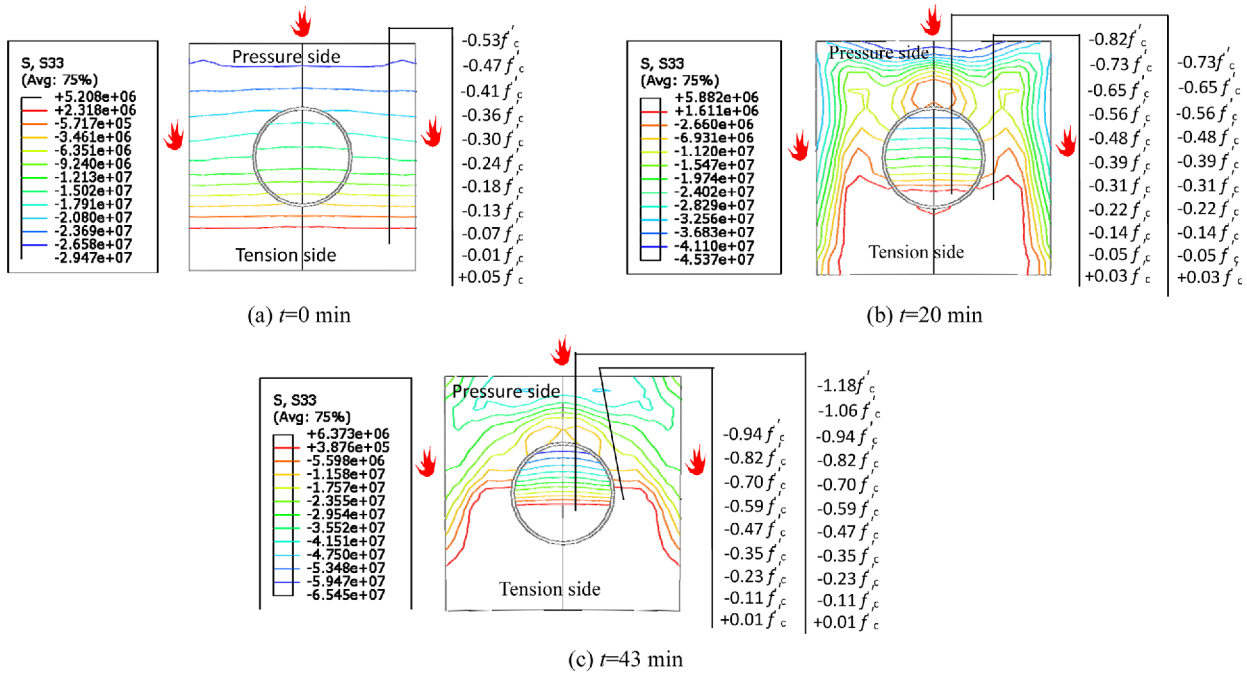


**Figure 13.** Development and change of longitudinal stress (S33) on mid-span section at different moments.

side presenting tension and the other side presenting compression. At the initial stage of the fire, the temperature of the peripheral reinforced concrete continually increased, which produced a certain amount of thermal expansion deformation. However, the loss of strength was not serious because of the relatively short fire exposing time. The outer reinforced concrete accepted the majority of the load and the compressive stress increasingly aggrandized such that the maximum compressive stress was collected at the edge of the compression section, as presented in Fig. 13(b). Following an increase in the fire time, the temperature of the external reinforced concrete further increased, the material performance rapidly deteriorated, the load of the external reinforced concrete decreased, so the compressive stress decreased. The load of the external reinforced concrete transferred to the section that exhibited a lower temperature, that was the section of internal concrete and concrete filled steel tube. The stress of the interior concrete and concrete filled steel tube gradually increased. In addition, the concrete filled steel tube exhibited a large compressive stress growth rate, such that the maximum compressive stress occurred in the interior periphery of the reinforced concrete and at the edge of concrete filled steel tube. Given the increase in the mid-height deflection of the CFSTRC columns, the area of the tensile zone gradually increased and the compression area decreased, such that the distribution of the longitudinal stress in the mid-height section no longer became even, as presented in Fig. 13(c).

(f) The contact stress between steel tube and concrete on mid-height sections

Under the combined action of external load and 3-side fire, the steel tube, which sandwiches between the outer reinforced concrete and inner core concrete, will produce contact stress in the contact zone and nearby. Figure 14 shows the contact stress between steel and concrete on mid-height sections of CFCTRC columns, where $P_1$ stands for the contact stress between peripheral concrete and steel tube, and $P_2$ denotes the contact stress between core concrete and steel tube, the unit of the contact stress is MPa. In the Figure 15 $P>0$ represents the existence of interaction between steel and concrete, and $P=0$ means steel tube and concrete happens interface separation.

According to Fig. 15(a), the steel and exterior concrete in tension side interacted due to the effect of the eccentric load on the column at normal temperatures, but the interaction at the compression side was equal to zero. At early fire times, the tension side was not exposed to fire, thereby resulting in slowly increasing interaction. As for the compression side, the interaction between the steel and exterior concrete was still equal to zero before about 20 min exposing time. After approximately 20 min, the steel tube and exterior concrete on the compression side interacted. Extensions in the heating time presented gradual increases in the contact stress ($P_1$) on both the pressure and tension sides. Following a heating time of 40 min, the value of $P_1$ obtained a peak value of 1.83 MPa. However, after the peak, the value of $P_1$ on both the

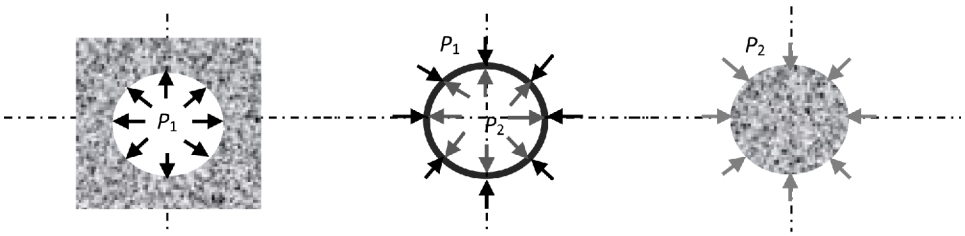


**Figure 14.** The sketch map of contact stress between steel tube and concrete on mid-height sections.

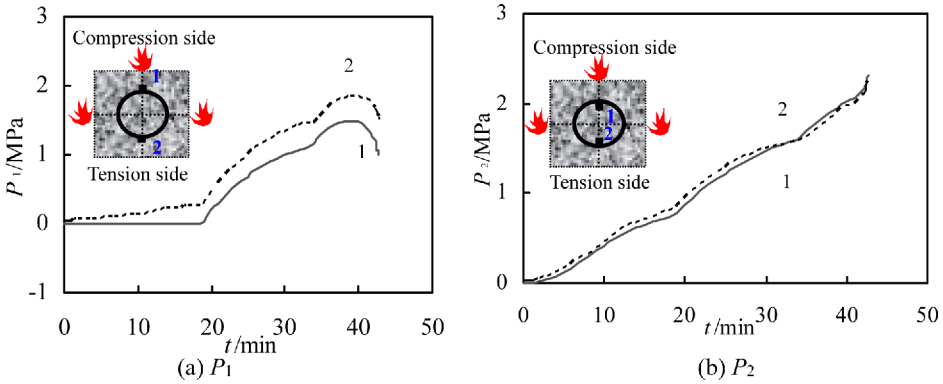


**Figure 15.** The contact stress-time curves between steel tube and concrete on mid-eight sections of CFSTRC columns.

pressure and tension sides sharply decreased.

Figure 15(b) presents the existence of interaction between the steel tube and core concrete at the beginning of the heating, where the contact stress was $P_2$>0. Following an increase in the fire time, the heat transferred to the interior, and the temperature of the core concrete filled steel tube continuously increased, such that the core concrete filled steel tube bore more load unloaded from external reinforced concrete, thereby exhibiting a gradual increasing contract deformation and transverse deformation. But the transverse deformation was restrained by external reinforced concrete, so the contract stress ($P_2$) increased gradually. When the columns failed, the interaction ($P_2$) exhibited a maximum value of 2.3 MPa.

## 4. Parameter Analysis

The CFSTRC columns presented a quite complicated working mechanism under the combined action of the load and three-sided fire, and there are many factors influenced the fire resistance of the CFSTRC columns. To fully understand the fire resistance of the three-sided fire-exposed CFSTRC columns, this section used the above-mentioned finite element analysis model to present a systematic analysis on influence of main parameters of the CFSTRC columns subjected to a three-sided fire. The parameters include fire load ratio ($n$), section size ($B$), slenderness ratio ($\lambda$), section core area ratio ($\alpha_{sc}=A_{sc}/A$, $A_{sc}$ is the cross-sectional area of concrete filled steel tube, $A$ is the total section area of CFSTRC columns), Section steel ratio ($\alpha_s=A_s/A_c$, $A_s$ is the area of section steel tube, $A_c$ is the area of core concrete), Load eccentricity ratio ($e/r_0$), Section reinforcement ratio ($\rho_b=A_{sb}/A_o$, $A_{sb}$ is the total cross-sectional area of longitudinal reinforcement, $A_o$ is the section area of external concrete), steel yield strength ($f_y$), concrete compression strength ($f_{cu}$).

The basic conditions of the same example are given in the 3.3 section, the ISO-834 (1999) international standard temperature versus time curve was used as an example to simulate fire for the analysis of the various parameters that affect the fire resistance ($t_R$) of the CFSTRC columns under three-side fire.

### 4.1. Fire load ratio ($n$) on $t_R$

Figure 16 presents the fire load ratio ($n$) effect on the fire resistance ($t_R$) of CFSTRC columns under three-side fire. The fire load ratio has a significant influence on the fire resistance CFSTRC columns under three-side fire, the larger the fire load ratio is, the lower the fire resistance is.

### 4.2. Section size($B$) on $t_R$

Figure 17 illustrates the variation of CFSTRC columns fire resistance under three-side fire with the section size ($B$). The section size has a great influence on the fire resistance of CFSTRC columns under three-side fire. An increase in the section size generated a fire resistance increase in the CFSTRC columns mainly due to an increase in the column section size. The larger volume of concrete strengthened the heat absorption capacity of the

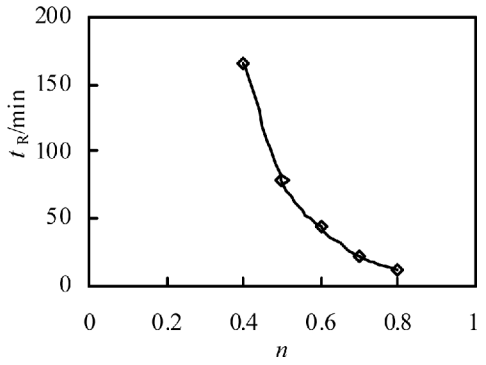


**Figure 16.** Fire load ratio effect on $t_R$.

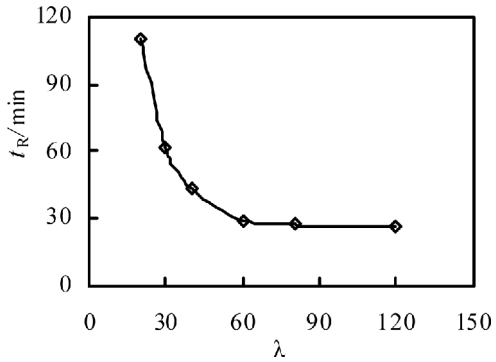


**Figure 18.** Slenderness ratio effect on $t_R$.

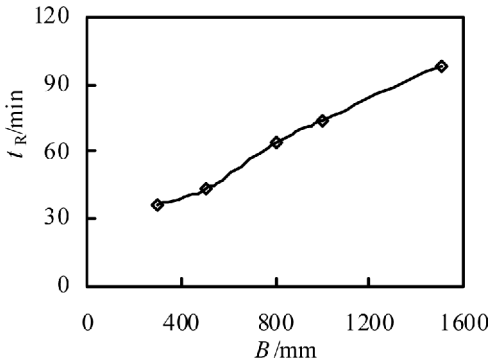


**Figure 17.** Section size effect on $t_R$.

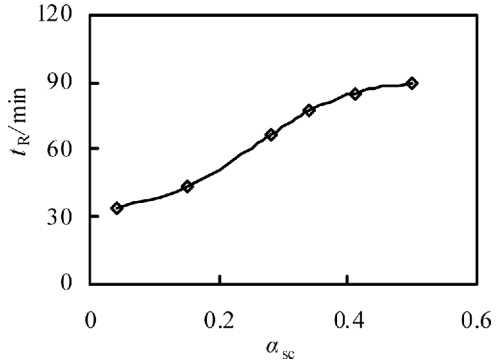


**Figure 19.** Section core area ratio effect on $t_R$.

column and slowed down the heat transfer rate, thereby increasing the refractory limit of the column in the presence of a three-sided fire. On the contrary, smaller section sizes presented smaller concrete capacities, which generated worse column heat absorption capacities and more rapidly heat transfer rate, resulting in smaller fire resistance in the three-sided fire-exposed CFSTRC columns.

### 4.3. Slenderness ratio ($\lambda$) on $t_R$

Figure 18 illustrates the slenderness ratio ($\lambda$) effect on the fire resistance ($t_R$) of CFSTRC columns under a three-sided fire. The slenderness ratio significant influenced the fire resistance of the three-sided fire-exposed CFSTRC columns. Bigger slenderness ratios presented more obvious two order effects and generated a lower fire resistance in the three-sided fire-exposed CFSTRC columns. When the slenderness ratio is larger than 60, the slenderness ratio has little influence on the fire resistance of the CFSTRC columns under three-side fire.

### 4.4. Section core area ratio ($\alpha_{sc}$) on $t_R$

Figure 19 shows the section core area ratio ($\alpha_{sc}$) effect on the fire resistance ($t_R$) of CFSTRC columns under three-side fire. The section core area ratio has a significant influence on the fire resistance CFSTRC columns. The larger section core area ratio increased the proportion of concrete filled steel tube, such that the fire resistance of CFSTRC columns under three-side fire increased.

### 4.5. Section steel ratio ($\alpha_s$) on $t_R$

Figure 20 illustrates the section steel ratio ($\alpha_s$) effect on the fire resistance ($t_R$) of CFSTRC columns under three-side fire. It can be found that the fire resistance increased with the enlargement of section steel ratio of CFSTRC columns. But in general, the section steel ratio has a less influence on the fire resistance of CFSTRC columns under three-side fire.

### 4.6. Load eccentricity ratio ($e/r_0$) on $t_R$

Figure 21 presents the load eccentricity ratio ($e/r_0$) effect on the fire resistance ($t_R$) of CFSTRC columns under three-side fire. The effect of load eccentricity ratio on the fire resistance of CFSTRC columns is not obvious.

### 4.7. Section reinforcement ratio ($\rho_b$) on $t_R$

Figure 22 shows the section reinforcement ratio ($\rho_b$) effect on the fire resistance ($t_R$) of CFSTRC columns under three-side fire. With the increasing of the section reinforcement ratio, the fire resistance of the CFSTRC columns increased. In general, the section reinforcement ratio has a little influence on the fire resistance of CFSTRC columns under three-side fire.

### 4.8. Steel yield strength ($f_y$) on $t_R$

Figure 23 illustrates the steel yield strength ($f_y$) effect on the fire resistance ($t_R$) of CFSTRC columns under three-side fire. It can be found from Fig. 20 that the fire

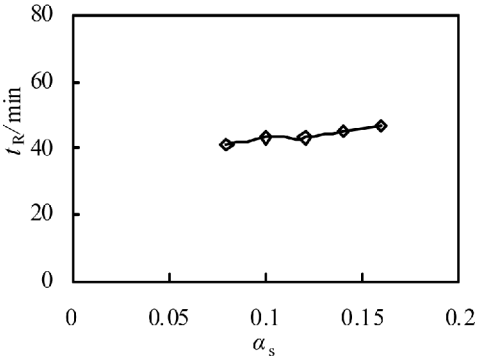


**Figure 20.** Section steel ratio effect on $t_R$

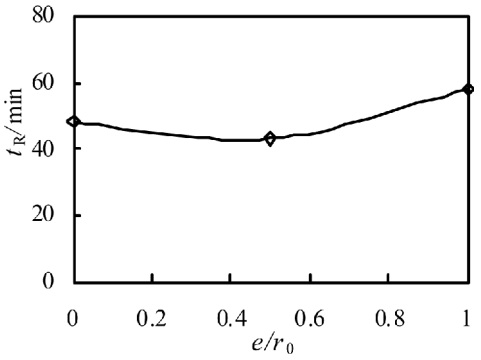


**Figure 21.** Load eccentricity ratio effect on $t_R$

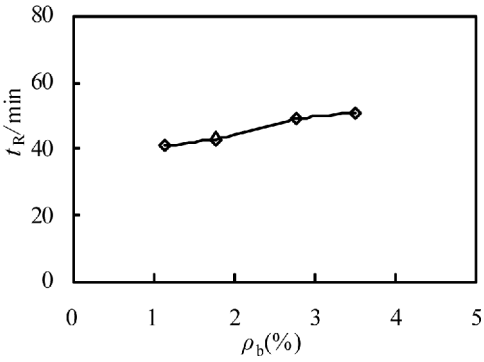


**Figure 22.** Section reinforcement ratio effect on $t_R$.

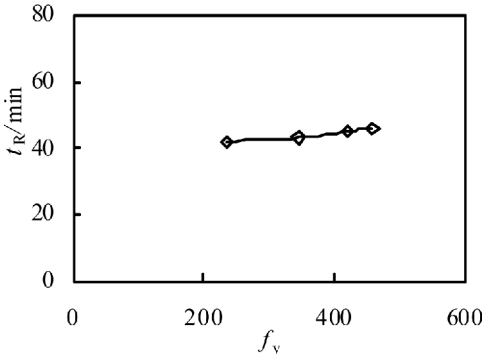


**Figure 23.** Steel yield strength effect on $t_R$.

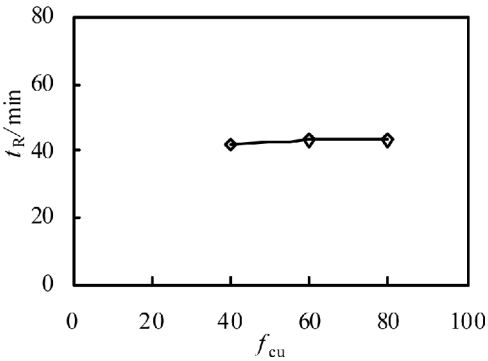


**Figure 24.** Core concrete compression strength effect on $t_R$.

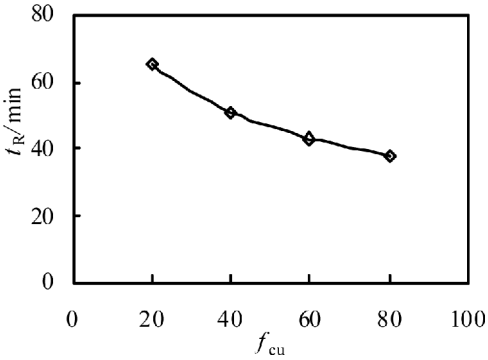


**Figure 25.** External concrete compression strength effect on $t_R$.

resistance increased with the increasing of the steel yield strength of CFSTRC columns. In general, the steel yield strength has less effect on the fire resistance of CFSTRC columns under three-side fire.

### 4.9. Core concrete compression strength ($f_{cu}$) on $t_R$

Figure 24 presents the core concrete compression strength ($f_{cu}$) effect on the fire resistance $t_R$ of CFSTRC columns under three-side fire. The core concrete compression has a little influence on the fire resistance of CFSTRC columns under three-side fire.

### 4.10. External concrete compression strength ($f_{cu}$) on $t_R$

Figure 25 illustrates the external concrete compression strength ($f_{cu}$) effect on the fire resistance ($t_R$) of CFSTRC columns under three-side fire. The external concrete compression strength significantly influenced the fire resistance of the three-sided fire-exposed CFSTRC columns. An increase in the compressive strength of the exterior concrete generated greater loss of the ultimate bearing capacity of the CFSTRC columns under high temperature, such that the CFSTRC columns decreased.

Based on Figs. 16 to 25, the section steel ratio ($\alpha_s$), load eccentricity ratio ($e/r_0$), cross-sectional reinforcement ratio ($\rho_b$), steel tube yield strength ($f_y$), and core concrete compression strength ($f_{cu}$) minimally impacted the fire resistance, whereas the fire load ratio ($n$), section size ($B$), slenderness ratio ($l$), section core area ratio ($a_{sc}$), and the

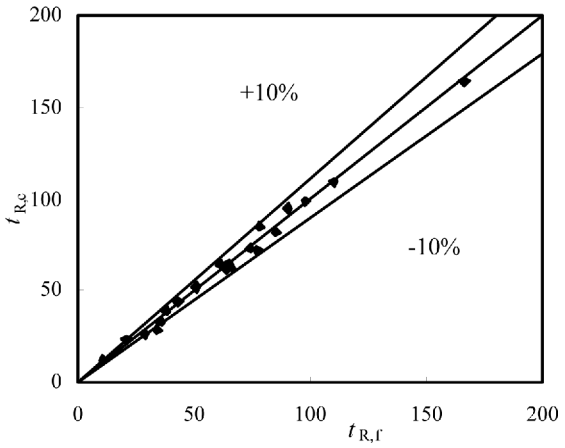


**Figure 26.** Comparison of $t_R$ between simplified results and numerical results.

external concrete compression strength ($f_{cu}$) greatly influenced the fire resistance of the CFSTRC columns Based on Figures 16 to 25, the section steel ratio ($\alpha_s$), load eccentricity ratio ($e/r_0$), cross-sectional reinforcement ratio ($\rho_b$), steel tube yield strength ($f_y$), and core concrete compression strength ($f_{cu}$) minimally impacted the fire resistance, whereas the fire load ratio ($n$), section size ($B$), slenderness ratio ($l$), section core area ratio ($a_{sc}$), and the external concrete compression strength ($f_{cu}$) greatly influenced the fire resistance of the CFSTRC columns under three-side fire.

## 5. Simplified Caculation

Based on the above analysis of the parameters, the present study determined the following parameter factors significantly influenced the fire resistance of the CFSTRC columns under three-side fire: the fire load ratio ($n$), section size cross section width ($B$), slenderness ratio ($l$), section core area ratio ($a_{sc}$), and the external concrete compression strength ($f_{cu}$). By considering the above five main factors as basic variables and limiting them in commonly used scope in practical engineering, the following conditions were assumed: a width of section ($B$) of 400-1500 mm, a steel ratio ($a_s$) of 0.04-0.2, a load eccentricity ($e/r_0$) of 0-1.0, a slenderness ratio ($l$) of 10-200, a steel yield strength ($f_y$) of 235-460 MPa, and a concrete cube strength ($f_{cu}$) of 30-100 MPa. The practical calculation formula of the fire resistance under a three-sided fire ($t_R$) was then obtained as follows:

$$t_R = \frac{3.851(-0.178B_0^2 + 5.134B_0 + 2.279)(-3.188\ln(f_{cu\,0}) + 7.588)(5.157\alpha_{sc\,0} + 5.476)}{e^{3.924n_0} \times \lambda^{1.292}} \quad (4)$$

$n_0=n/0.6$, $B_0=B/500$, $\lambda_0=\lambda/40$, $\alpha_{sc0}=\alpha_{sc}/0.15$, $f_{cu0}=f_{cu}/60$.

where $n$ represents the fire load ratio, $B$ represents the cross section size in mm, $l$ represents the slenderness ratio, $a_{sc}$ represents the section core area ratio, and $f_{cu}$ represents the external concrete compression strength.

Figure 26 presents the comparison between the simplified calculation results and the finite element analysis results of the fire resistance, $t_R$, of the CFSTRC columns under three-side fire, where $t_{R,f}$ and $t_{R,c}$ represent the finite element analysis results and the simplified calculation results, respectively. The calculated results were in well agreement with the finite element results.

## 6. Conclusions

The present study characterized the mechanical behavior of concrete filled steel tube reinforced concrete (CFSTRC) columns subjected to 3-side fire. Based on the research stated in the paper, the following conclusions can be drawn:

(1) The CFSTRC columns subjected to 3-side fire exhibited a mono-symmetrical thermal distribution and a significantly lower temperature on the side unexposed to fire as compared to the surface exposed to fire. At the end of the heating, the maximum temperature difference can reach as high as 1065°C. The large temperature difference resulted in non-uniform thermal stress and strain in the cross section, thereby generating an eccentric rotation of intensity at the center of the cross section.

(2) The existence of concrete inside and outside of the steel tube effectively prevented the generation of local buckling within the steel tube. In addition, the failure modes of the CFSTRC columns exhibited overall bucking after the column reached its fire endurance.

(3) The fire load ratio, cross-section size, slenderness ratio, section core area ratio, and exterior concrete compression strength significantly affected the fire resistance of the CFSTRC columns under three-side fire..

(4) A simplified calculation formula for the fire resistance of the CFSTRC columns under three-side fire was proposed based on the analysis of the parameters. The simplified calculation results were verified using the finite element analysis results, wherein the validation indicated that the simplified calculation formula provided a more convenient and feasible method of computing the fire resistance of the component under three-side fire. These results can be referenced for fire resistance designs in practical engineering.

## Acknowledgments

The research reported in the paper is part of the Project 51378094 supported by National Natural Science Foundation of China and the Project 2013020107 supported by

National Natural Science Foundation of Liaoning Province, and the Fundamental Research Funds for the Central Universities (China) (DC201502040201). The financial supports are highly appreciated.

## References

Feng Y.H., Shen T., Lou W.J. and Zhou J. (2008). "The study of residual load bearing capacity of column reinforced by Inner circular steel tube after fire." *Industrial Construction*, 38(3), pp. 16-19. (in Chinese)

Guo Z.H and Shi X.D. (2003). "Behaviour of reinforced concrete at elevated temperature and its calculation." *Beijing: Tsinghua University Press,* 2003: pp. 40-42. (in Chinese)

Han, L.H. (2007). *Concrete Filled Steel Tubular Structures-Theory and Practice*. Science Press, BeiJing, B.J., China. (in Chinese)

Hong, Z. and Tao, Z. (2005). "Review of research on RC columns reinforced with concrete filled steel tubes in China." *Journal of Fuzhou University (Natural Science)*, 33(sup), pp. 316-320. (in Chinese)

Hibbitt, Karlson, Sorenson., 2007. "ABAQUS Version 6.7: Theory manual, user's manual, verification manual and example problems manual." *Hibbit, Karlson and Sorenson Inc.*

ISO 834-1 (1999). Fire resistance tests-elements of building construction: Part 1: general requirements [S]. Geneva, Switzerland: International Organization for Standardization

Li L.L. (2011). "Fire resistance of steel reinforced concrete (SRC) columns subjected to small eccentric load and 3-side fire exposure." *Master Dissertation of Suzhou University of Science and Technology.* (in Chinese)

Li, M.F. (2003). "Fire Resistance Behaviour and Design of Steel Column with Restraint of Wall Panels" *Shanghai: Tongji University.* (in Chinese)

Lie, T.T., Lin, T.D., Allen, D.E. and Abrams, M.S. (1984). "Fire resistance of reinforced concrete columns." *NRC-CNRC Internal Report*, NO. 1167, Canada.

Lie T.T. and Chabot M. (1992). "Experimental Studies on the Fire Resistance of Hollow Steel Columns Filled with Plain Concrete." *NRC-CNRC Internal Report*, No.611, Canada.

Lie T.T. and Denham E.M. (1993). "Factors Affecting the Fire Resistance of Circular Hollow Steel Columns Filled with Bar-reinforced Concrete." *NRC-CNRC Internal Report*, No.651, Canada.

Lie T.T. (1994). "Fire resistance of circular steel columns filled with bar-reinforced concrete." *Journal of Structural Engineering*, ASCE, 120(5), pp. 1489-1509.

Lv, X.T., Yang, H. and Zhang S.M. (2012). "Fire resistance limit of concrete-filled square steel tube columns exposed to three-faced fire." *Journal of Natural Disasters*, 21(3), pp. 198-203. (in Chinese)

Lv, X.T., Yang, H. and Zhang S.M. (2012). "Fire resistance limit of concrete-filled square hollow sections being exposure to two-opposite fire." *Industial Construction*, 42(6), pp. 148-152. (in Chinese)

Lv, X.T., Yang, H. and Zhang S.M. (2013). "Fire resistance behavior and mechanism of concrete filled square hollow columns in non-uniform fires." *Journal of Building Structures*, 34(3), pp. 35-44. (in Chinese)

Lv, X.T. (2010). "Fire Resistance Behavior and Design of Concrete-Filled SHS in Non-uniform Fires." *Harbin industrial university PhD thesis*. (in Chinese)

Liu, F.Q. (2010). "Fire Resistance of concrete filled RHS columns under three-surface fire loading." *Harbin industrial university PhD thesis*. (in Chinese)

Wu B., Tang G.H. and Wang, C. (2007). "Experimental study on fire resistance of RC columns with different faces exposed to fire" *China Civil Engineering Journal*, 40(4), pp. 27-31. (in Chinese)

Xu, L. and Liu, Y.B. (2013). "Concrete filled steel tube reinforced concrete (CFSTRC) columns subjected to ISO-834 standard fire: experiment." *Advances in Structural Engineering*, 16(7), pp. 1263-1282.

Yang, H., Lv, X.T. and Zhang S.M. (2010). "Temperature distributions of concrete-filled steel tubes with rectangular sections while exposure to one-side fire." *Journal of Tianjin University*, 43(5), pp. 392-399. (in Chinese)